# Analytical approach to viscous fingering in a cylindrical Hele-Shaw cell

José A. Miranda*
*Laboratório de Física Teórica e Computacional, Departamento de Física, Universidade Federal de Pernambuco, Recife, PE 50670-901 Brazil*

(Received 20 August 2001; published 15 January 2002)

We report analytical results for the development of the viscous fingering instability in a cylindrical Hele-Shaw cell of radius $a$ and thickness $b$. We derive a generalized version of Darcy's law in such cylindrical background, and find it recovers the usual Darcy's law for flow in flat, rectangular cells, with corrections of higher order in $b/a$. We focus our interest on the influence of the cell's radius of curvature on the instability characteristics. Linear and slightly nonlinear flow regimes are studied through a mode-coupling analysis. Our analytical results reveal that linear growth rates and finger competition are inhibited for an increasingly larger radius of curvature. The absence of tip-splitting events in cylindrical cells is also discussed.

DOI: 10.1103/PhysRevE.65.026303 PACS number(s): 47.20.Ma, 47.60.+i, 47.20.Ky, 47.54.+r

## I. INTRODUCTION

When a fluid is pushed by a less viscous one in a narrow space between two parallel plates (a device known as Hele-Shaw cell), the Saffman-Taylor instability arises [1]. This hydrodynamic instability results in the complex evolution of the moving interface between the fluids, producing a wide range of patterns [2]. Since the pioneering work of Saffman and Taylor [1], these visually striking, viscous fingering patterns have been extensively studied, both theoretically and experimentally [2].

One noteworthy distinction between experimental and theoretical work on the Saffman-Taylor problem is that the measurements usually reveal disturbances associated with friction at the sidewalls of the Hele-Shaw cell, while most theoretical studies sidestep this problem by assuming periodic boundary conditions. In principle, rigid-wall boundary conditions would be closer to an experimental realization of the problem. However, the use of periodic boundary conditions, as opposed to rigid-wall ones in theoretical investigations of the Saffman-Taylor problem has been a matter of interest and debate during the last few decades [2–6].

In the early 1990's, an attempt to measure the flow in a cell that approximates the periodic boundary conditions of the theory has been performed by Zhao and Maher [5]. Their interesting experimental work considered gravity-driven viscous flow within a *cylindrical* Hele-Shaw cell (two coaxial cylinders separated by a small gap) of large radius of curvature. To drive the system gravitationally, they allowed the fluids to form a stable flat interface, and then invert the cell to put the denser fluid on the top. The fluids used in [5] had almost the same viscosity (low-viscosity contrast), such that the process of finger competition leads to a nearly up-down symmetric interface. The main goal in Ref. [5] was to directly compare viscous fingering flow in a cylindrical cell with flow in a conventional, flat, rectangular cell, and verify if the rigid sidewalls could be viewed as having been replaced with periodic boundary conditions.

Comparison of the pattern evolution observed in the cylindrical cell experiment [5] with similar measurements in rectangular cells with sidewalls [7,8], shows that periodic boundary conditions yield *few differences* of results. Moreover, the cylindrical cell patterns also look very similar to computer simulation results obtained by Tryggvason and Aref [4], who used periodic boundary conditions in a flat rectangular cell.

The experimental results presented in [5] suggest that, for a large radius of curvature and low-viscosity contrast, there are no significant changes made in the statistical properties of the Saffman-Taylor flow by friction at the boundaries. In other words, it seems that the boundaries affect the dynamics in much the same way whether they are provided by periodic boundary conditions or by the presence of physical sidewalls. Although the majority of flow features survive the elimination of sidewall friction, the authors in Ref. [5] were not able to perform a meaningful test of growth rates in the linear regime due to experimental disturbances other than rigid-wall ones, related to the inversion of the cell. It is worth noting that sidewall effects are more prominent in cases with higher-viscosity contrast [9–11].

Despite the relevance and simplicity of the experimental work carried out in Ref. [5], a theoretical analysis of the viscous fingering instability in a cylindrical Hele-Shaw cell is lacking in the literature. A theoretical study of flow in cylindrical cells, could yield insight into the possible causes that may contribute to the few differences of results detected in [5]. In this paper, we examine flow in cylindrical cells analytically. We consider the general case of arbitrary viscosity contrast and cell radius. In Sec. II, we derive a generalized version of Darcy's law suitable to describe flow in cylindrical cells. This version introduces a correction factor, which depends on the ratio between the cell's thickness and radius. This result enables us to express the differences of behavior between flow in rectangular and cylindrical cells in quantitative terms. In Sec. III, we investigate the consequences of such differences in the flow dynamics by performing a mode-coupling analysis of the problem. We examine both linear and slightly nonlinear stages of evolution, and explicity show how linear growth rates and the dynamical process of finger competition are influenced by cylindrical geometry. The absence of finger tip splitting in cylindrical

*E-mail address: jme@lftc.ufpe.br

 

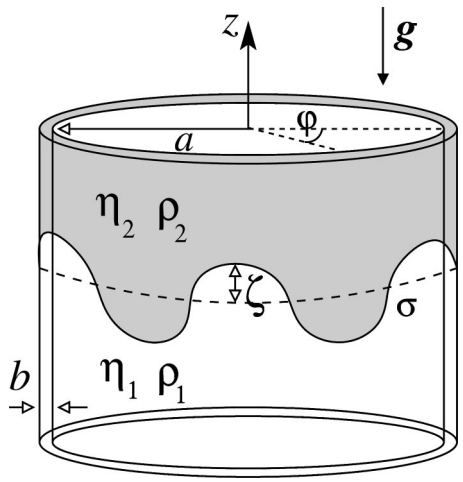


FIG. 1. Schematic configuration of viscous flow in a cylindrical Hele-Shaw cell. The dashed curve represents the unperturbed interface $z=0$, and the solid undulated curve depicts the perturbed interface $z=\zeta(\varphi,t)$. All other relevant quantities are defined in the text.

cells is briefly discussed. Section IV presents our final remarks.

## II. DARCY'S LAW IN CYLINDRICAL ENCLOSURES

In this section, we present the physical system of interest and derive a generalized Darcy's law that is suited to bringing out the geometrical aspects related to viscous fluid flow in cylindrical passages. Consider two immiscible, incompressible, viscous fluids, flowing in a narrow gap of thickness $b$, between two long coaxial, thin right circular cylinders (cylindrical Hele-Shaw cell). The radius of curvature of the cylindrical cell is $a$ (see Fig. 1). Denote the densities and viscosities of the lower and upper fluids, respectively, as $\rho_1, \eta_1$ and $\rho_2, \eta_2$. The flows in fluids 1 and 2 are assumed to be irrotational, and between them there exists a surface tension $\sigma$. The acceleration of gravity is represented by $\mathbf{g}$, and points downward along the direction of the cylinders' common axis.

In order to derive a generalized version of Darcy's law, adjusted to describe flow in such confined cylindrical environment, it suffices to focus on a single fluid. The starting point of our calculation is a coordinate-free representation of the continuity equation for an incompressible fluid

$$\boldsymbol{\nabla}\cdot\mathbf{u}=0, \tag{1}$$

and the Navier-Stokes equation

$$\rho\left[\frac{\partial\mathbf{u}}{\partial t}+(\mathbf{u}\cdot\boldsymbol{\nabla})\mathbf{u}\right]=-\boldsymbol{\nabla}p+\eta\boldsymbol{\nabla}^2\mathbf{u}+\rho\mathbf{g}, \tag{2}$$

where $\mathbf{u}$ denotes the three-dimensional fluid velocity and $p$ is the hydrodynamic pressure.

We consider cylindrical coordinates $(r,\varphi,z)$, where the $z$ axis coincides with that of the two cylinders. Specializing to the case of flow in the $z$ direction $\mathbf{u}_z(r,z)=u_z(r,z)\hat{\mathbf{z}}$, the continuity Eq. (1) leads to $\partial(r\ u_z)/\partial z=0$. Consequently, the velocity may be written is a function of $r$ only

$$\mathbf{u}_z=u(r)\ \hat{\mathbf{z}}, \tag{3}$$

where $\hat{\mathbf{z}}$ denotes the unit vector along the $z$ axis.

Following the standard approach in Hele-Shaw problems, we restrict our attention to small-velocity flows of viscous fluids, and neglect the inertial terms on the left-hand side of Eq. (2). Under such circumstances, we use the solution (3) to rewrite the Navier-Stokes equation as

$$\frac{\partial p}{\partial z}-\rho g=\frac{\eta}{r}\ \frac{\partial}{\partial r}\left[r\frac{\partial\ u(r)}{\partial r}\right]. \tag{4}$$

Since the left-hand side is a function of $z$, and the right-hand side involves only $r$, Eq. (4) may be satisfied only if each side is equal to a constant of common value $B$. Imposing the no-slip boundary conditions at the solid cylindrical shells $u(a)=u(a+b)=0$, we find the solution of the radial equation

$$u(r)=\frac{B}{4\eta}\left[r^2-C\log\left(\frac{r}{a}\right)-a^2\right], \tag{5}$$

where $C=[(a+b)^2-a^2]/\log(1+b/a)$. In contrast to flow in usual flat, rectangular cells, observe that the velocity profile Eq. (5) is not rigorously parabolic (or, Poiseuille-like) due to the presence of a logarithmic term. The profile is very close to a parabola for $r/a\ll 1$, but deviates from parabolic shape for larger values of $r/a$.

Averaging the three-dimensional velocity $\mathbf{u}$ with respect to the transverse, radial direction, defining $v\equiv(1/b)\ \int_a^{a+b}u(r)dr$, leads to the equation for the mean flow velocity of the fluid

$$v=-\frac{b^2\ F(b/a)}{12\eta}\left[\frac{\partial p}{\partial z}-\rho g\right], \tag{6}$$

where

$$F(b/a)=3\left(\frac{a}{b}\right)^3\left\{\frac{\frac{b}{a}\left[1-\left(1+\frac{b}{a}\right)^2\right]}{\log\left(1+\frac{b}{a}\right)}-\frac{2}{3}\left[1-\left(1+\frac{b}{a}\right)^3\right]\right\}. \tag{7}$$

Equation (6) is Darcy's law for flow in cylindrical Hele-Shaw cells. The function $F(b/a)\approx 1+(1/30)(b/a)^2+O((b/a)^3)$ introduces a correction factor that measures the deviation from the flat, rectangular case $(a\to\infty)$. Equation (6) recovers the usual Darcy's law for flow in flat cells with corrections of higher order in $b/a$, introduced by $1\leqslant F(b/a)\leqslant 2$.

Darcy's law is the governing equation for Hele-Shaw-type flows [2]. Therefore, quantitative comparisons between dynamical behavior of flow in rectangular and cylindrical cells must take into account the corrections introduced by Eq. (6), in addition to those caused by sidewall effects and cell in-

version [5]. In contrast to the unavoidable disturbances mentioned in Ref. [5], which are hard to quantify accurately, Eq. (6) allows precise determination of intrinsic, purely geometrical effects.

Based on Eq. (7), we may start understanding why the differences of results detected in Ref. [5] were so small. In Ref. [5], the authors used a cylindrical cell of radius of curvature $a=18$ mm and thickness $b=1$ mm, such that $b/a \approx 5.6\times 10^{-2}$. From Eq. (7), this means a small correction of 0.01% with respect to the flat cell case ($a\to\infty$). In practical terms, we estimate that a ratio of roughly $b/a\approx 10^{-3}$ would be enough in order for curvature effects to be considered negligible.

### III. LINEAR AND SLIGHTLY NONLINEAR DYNAMICS

In this section, we investigate the consequences of the changes introduced by the generalized Darcy's law (6) in both linear and weakly nonlinear stages of the interface evolution. We focus on two general questions: (i) On the linear level, what is the effect of Eq. (6) on linear growth rates? (ii) Concerning the onset of nonlinear effects, how are finger competition, up-down interfacial symmetry, and finger tip splitting influenced by Eq. (6)?

To study these issues, we derive a second-order mode-coupling differential equation for the interface perturbation amplitudes. We express the fluid-fluid interface as a Fourier series

$$\zeta(\varphi,t)=\sum_{n=-\infty}^{+\infty}\zeta_n(t)\exp(in\varphi), \tag{8}$$

where $\zeta_n(t)$ denotes the complex Fourier mode amplitudes and $n=0,\pm 1,\pm 2,\ldots$, is the discrete azimuthal wave number.

We exploit the irrotational flow condition to define the velocity potential $\mathbf{v}_j=-\boldsymbol{\nabla}\phi_j$ in fluids $j=1$ and 2. Using the velocity potential, we evaluate Darcy's law (6) for each of the fluids on the interface, subtract the resulting expressions from each other, and divide by the sum of the two fluids' viscosities to get the equation of motion

$$A\left(\frac{\phi_1|_\zeta+\phi_2|_\zeta}{2}\right)-\left(\frac{\phi_1|_\zeta-\phi_2|_\zeta}{2}\right)=F(b/a)[Uz+\kappa]|_\zeta. \tag{9}$$

Note the presence of the correction factor (7) on the right-hand side of Eq. (9). To obtain Eq. (9) we used the pressure boundary condition $p_2-p_1=\sigma\kappa$ at the interface $z=\zeta$, where $\kappa=(1/a^2)(\partial^2\zeta/\partial\varphi^2)[1+(\partial\zeta/\partial\varphi)^2]^{-3/2}$ is the interfacial curvature. The viscosity contrast $\mathrm{A}=(\eta_2-\eta_1)/(\eta_2+\eta_1)$, and $U=b^2g(\rho_2-\rho_1)/[12(\eta_1+\eta_2)]$ is a characteristic velocity. In Eq. (9), we introduced dimensionless variables, scaling all lengths by the gap-size $b$, and all velocities by $\sigma/12(\eta_1+\eta_2)$. From now on we work, unless otherwise stated, with the dimensionless version of Eq. (9).

Following steps similar to those performed in [12–14], we define Fourier expansions for the velocity potentials

$$\phi_j=\sum_{n\neq 0}\phi_{jn}(t)\exp\left[in\varphi+(-1)^{j-1}\frac{|n|}{a}z\right], \tag{10}$$

which obey Laplace's equation and vanish as $z\to\pm\infty$. We express $\phi_j$ in terms of the perturbation amplitudes $\zeta_n$ by considering the kinematic boundary condition for flow in a cylindrical cell. As in the flat cell case, the kinematic condition $\mathbf{n}\cdot\mathbf{v}_1|_{z=\zeta}=\mathbf{n}\cdot\mathbf{v}_2|_{z=\zeta}$ refers to the continuity of the normal velocity across the fluid-fluid interface. Substituting these relations into Eq. (9), and Fourier transforming, yields the mode-coupling equation of the Saffman-Taylor problem in a cylindrical Hele-Shaw cell

$$\dot{\zeta}_k=\lambda(k)\zeta_k+\sum_{k'\neq 0}G(k,k')\dot{\zeta}_{k'}\zeta_{k-k'}+O(\zeta_k^3), \tag{11}$$

conveniently written in terms of the characteristic wavenumber $k=n/a$. The overdot denotes total time derivative, and

$$\lambda(k)=F(b/a)|k|[U-k^2] \tag{12}$$

is the dimensionless linear growth rate. The function

$$G(k,k')=A|k|[1-\mathrm{sgn}(kk')] \tag{13}$$

is the second-order mode-coupling term, where the sgn function equals $\pm 1$ according to the sign of its argument.

Based on mode-coupling Eq. (11), we now discuss some noteworthy features of both linear and weakly nonlinear regimes. Start with the linear growth rate (12): it is written as the product of the correction factor $F(b/a)$ by $\lambda(k)_{rect}=|k|[U-k^2]$, which incidentally, is the linear growth rate for the flat, rectangular case [12]. This last observation indicates that, for fixed gap-thickness $b$, there is a slight decrease of linear growth for increasingly larger radius of curvature $a$. The linear solution to Eq. (11) is purely exponential $\zeta_k^{lin}(t)=\zeta_k(0)\exp[\lambda(k)t]$, and introduces the correction factor $F(b/a)$ into the linear, rectangular solution [12]. At the linear level, this correction becomes more and more important as time progresses and when $b/a\to 1$.

From Eq. (12), we may extract two relevant parameters: (i) the critical wave-number $k_c=1/\sqrt{U}$ [defined by setting $\lambda(k)=0$], beyond which all modes are linearly stable; and (ii) the fastest growing mode $k^*=k_c/\sqrt{3}$, which maximizes $\lambda(k)$, and dominates the initial dynamics of the interface. Note that $k_c$ and $k^*$ show no dependence on the radius of curvature $a$. This behavior is illustrated in Fig. 2, which depicts the linear growth rate (12) as a function of $k$, in the flat cell limit (dashed curve) and for a cylindrical cell with $a\approx b$ (solid curve). Note that for both cases, the peak location and width of the band of unstable modes remain unchanged, independently of the value of $a$. Differences in behavior between flow in cylindrical and flat cells are more pronounced around $k^*$. These facts may be interpreted as follows: since $k=n/a$, if one increases the cell's radius of curvature $a$, the number of fingers $n$ at the two-fluid interface is also increased in order to keep the fastest-growing $k$ constant.

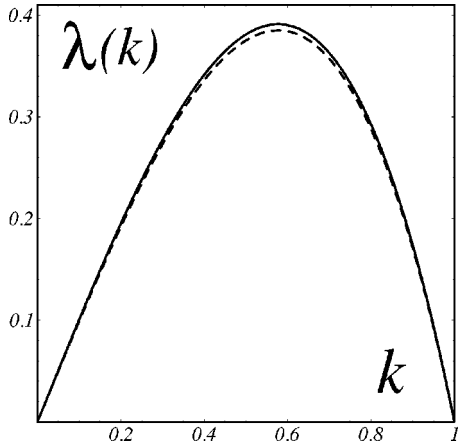


FIG. 2. Variation of the dimensionless growth rate (12) as a function of $k$, for $U=1$: in the flat cell limit $b/a\to 0$ (dashed curve), and in the cylindrical case $b/a\to 1$ (solid curve). Note that for both situations, $k_c=1$ and $k^*=1/\sqrt{3}$.

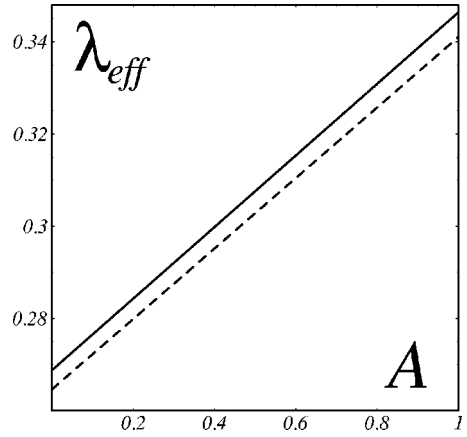


FIG. 3. Variation of the effective growth rate $\lambda_{eff}=\lambda(k_s)[1+Ak_sa_{k_f}]$, from Eq. (14), as a function of $A$, for $U=1$ and $a_{k_f}=1$: in the flat cell limit $b/a\to 0$ (dashed line), and in the cylindrical case $b/a\to 1$ (solid line). For a given value of viscosity contrast $A$, finger competition increases for larger values of $b/a$.

Now we turn our attention to the weakly nonlinear flow stage. We begin by discussing finger-competition dynamics. It is well known that the viscosity contrast $A$ has a crucial role in determining interfacial behavior for flow in flat rectangular cells [4,5,7,8,12]. For low-viscosity contrast ($A\approx 0$), the interface is nearly up-down symmetric, and increasingly larger asymmetry is observed for larger values of $A(A\approx\pm 1)$. Consequently, $A$ has great influence on the dynamics of finger competition and pattern selection. In cylindrical cells, in addition to the parameter $A$, it is of interest to examine how finger-competition dynamics is affected by radius of curvature $a$ (or correspondingly, by the correction factor $F(b/a)$).

In order to investigate finger competition, we consider the influence of a fundamental mode, on the growth of its subharmonic. To do that we rewrite the net perturbation (8) in terms of cosine and sine modes, where the cosine $a_k=\zeta_k+\zeta_{-k}$ and sine $b_k=i(\zeta_k-\zeta_{-k})$ amplitudes are real valued. Then, for consistent second-order expressions, we replace the time-derivative terms $\dot{a}_k$ and $\dot{b}_k$ on the right-hand side of Eq. (11) by $\lambda(k)a_k$ and $\lambda(k)b_k$, respectively. We consider a dominant fundamental of wave-number $k_f=k^*$, and a subharmonic of wave-number $k_s=k_f/2$ and relatively weaker amplitude. Without loss of generality, we may take $a_{k_f}>0$ and $b_{k_f}=0$. Under these circumstances, we obtain the following equations of motion for sine and cosine subharmonic:

$$\dot{a}_{k_s}=\lambda(k_s)[1+Ak_sa_{k_f}]a_{k_s}, \tag{14}$$

$$\dot{b}_{k_s}=\lambda(k_s)[1-Ak_sa_{k_f}]b_{k_s}. \tag{15}$$

Note that if $A>0$ and $a_{k_f}>0$, the fundamental accelerates the growth of the subharmonic cosine and inhibits the subharmonic sine mode. This causes increased variability among the lengths of fingers of less viscous fluid 1 penetrating more viscous fluid 2. This effect describes finger competition. As they were in flat cells, interface asymmetry and finger competition are enhanced to a degree proportional to $A$.

Although the second-order term $G(k,k')$ [see Eq. (13)] has no explicit dependence on $a$, the coupling between modes $k_f$ and $k_s$ makes the interface dynamics sensitive to the background cylindrical geometry. From Eqs. (14) and (15), we see that for a given $A$, the degree of competition and up-down asymmetry depend on the overall multiplicative term $\lambda(k_s)$, which in turn is proportional to the correction factor $F(b/a)$. To illustrate the combined influence of $A$ and $a$ on finger competition, we plot in Fig. 3 the effective growth rate $\lambda_{eff}=\lambda(k_s)[1+Ak_sa_{k_f}]$, taken from Eq. (14), as a function of viscosity contrast $A$. In Fig. 3, the dashed line corresponds to the flat cell limit, while the solid line expresses behavior for a cylindrical cell with $a\approx b$. We see from Fig. 3 that the discrepancies between flow in cylindrical and flat cells are more noticeable for increasingly larger values of *both* $A$ and $b/a$. Therefore, with respect to finger competition, the flow will be more stable with the increase of the cylindrical cell radius $a$. Geometrically speaking, we can say that the mean curvature $H=(1/2a)$ of the cylindrical cell intensifies the competition among fingers in comparison with that of rectangular, planar flow.

We conclude this section by briefly discussing the possibility of occurrence of finger tip splitting in cylindrical cells. Tip splitting is related to the influence of a fundamental mode $k_f$ on the growth of its harmonic $k_h=2k_f$ [12]. By rewriting Eq. (11) in terms of sine and cosine modes, and considering the coupling between $k_f$ and $k_h$, we verify that the harmonic mode cannot be influenced by the fundamental. Therefore, at second order, there is no tendency for the fingers to split in cylindrical cells. Tip splitting is absent for any value of the cell's radius of curvature $a$, including the flat cell limit $a\to\infty$. This fact may be interpreted in geometric terms as follows: unlike finger-competition behavior, which depends on, and varies with the cylinder's *mean* curvature $H$, finger tip splitting is controlled by *Gaussian* curvature [14], which is zero for a cylinder. In this sence, the absence of tip splitting in cylindrical cells was expected.

## IV. CONCLUSIONS AND PERSPECTIVES

In this paper, we investigated viscous flow in cylindrical Hele-Shaw cells analytically. The study of flow in such geometry requires modification of Darcy's law equation. A generalized version of Darcy's law was derived from first principles. It introduces pertinent corrections to the usual version of Darcy's law in flat, rectangular geometry. We used a mode-coupling approach to examine the fluid-fluid interface evolution. Arbitrary viscosity contrast $A$ and cell radius $a$ have been considered. We deduced the following general results: On the linear level, there is an inhibition of growth for increasingly larger radius of curvature $a$; and, for sligthly nonlinear stages, we found that finger competition and interface asymmetry are enhanced for flow in cylindrical cells. In addition, we explained the absence of tip-splitting events in cylindrical cells.

The study of geometry-related corrections $F(b/a)$ for the case $b/a>1$ could be interesting to study in the future. Within this limit, and following the lines of recent work by Ruyer-Quil [15] and by Meignin *et al.* [16], it would be of interest to study inertial corrections to the generalized Darcy's law (6), and examine gap-size effects for the Saffman-Taylor instability in cylindrical cells. Experimental study in this direction could use, and take advantage of already existing, very good cylindrical Taylor-Couette cells. In addition, a thorough investigation of fully nonlinear flow stages in cylindrical cells, through extensive computer simulations, may reveal additional corrections and dynamic behavior. Such numerical studies could provide a more meaningful confrontation between experiment and theory in cylindrical cells.

## ACKNOWLEDGMENTS

I thank CNPq and FINEP (through its PRONEX Program) for financial support. Helpful discussions with Fernando Parisio and Claudio Furtado are gratefully acknowledged.

[1] P.G. Saffman and G.I. Taylor, Proc. R. Soc. London, Ser. A **245**, 312 (1958).
[2] For review articles on this subject, see D. Bensimon, L.P. Kadanoff, S. Liang, B.I. Shraiman, and C. Tang, Rev. Mod. Phys. **58**, 977 (1986); G. Homsy, Annu. Rev. Fluid Mech. **19**, 271 (1987); K.V. McCloud and J.V. Maher, Phys. Rep. **260**, 139 (1995).
[3] B.W. Thompson, J. Fluid Mech. **31**, 379 (1968).
[4] G. Tryggvason and H. Aref, J. Fluid Mech. **136**, 1 (1983).
[5] H. Zhao and J.V. Maher, Phys. Rev. A **42**, 5894 (1990).
[6] F.X. Magdaleno and J. Casademunt, Phys. Rev. E **63**, 043102 (2001), and references therein.
[7] M.W. DiFrancesco and J.V. Maher, Phys. Rev. A **39**, 4709 (1989).
[8] M.W. DiFrancesco and J.V. Maher, Phys. Rev. A **40**, 295 (1989).
[9] C.W. Park and G.M. Homsy, J. Fluid Mech. **139**, 291 (1984).
[10] J.V. Maher, Phys. Rev. Lett. **54**, 1498 (1985).
[11] T. Maxworthy, J. Fluid Mech. **177**, 207 (1987).
[12] J.A. Miranda and M. Widom, Int. J. Mod. Phys. B **12**, 931 (1998).
[13] J.A. Miranda, F. Parisio, F. Moraes, and M. Widom, Phys. Rev. E **63**, 016311 (2001).
[14] F. Parisio, F. Moraes, J.A. Miranda, and M. Widom, Phys. Rev. E **63**, 036307 (2001).
[15] C. Ruyer-Quil, C. R. Acad. Sci., Ser. IIb: Mec., Phys., Chim., Astron. **329**, 1 (2001).
[16] L. Meignin, P. Ern, P. Gondret, and M. Rabaud, Phys. Rev. E **64**, 026308 (2001).